Presented at "The 4th European Conference on Antennas and Propagation" (EuCAP 2010), Barcelona, Spain, 12-16 April 2010.

An Accurate and Efficient Error Predictor Tool for CATR Measurements

C. Cappellin[#], S. Busk Sørensen[#], M. Paquay[+], A. Østergaard[+]

[#]*TICRA, Læderstræde 34, 1201 Copenhagen, Denmark*
{cc, sbs}@ticra.com

[+] *ESTEC, European Space Research and Technology Centre, Keplerlaan 1*
2201 Noordwijk, The Netherlands
{Maurice.Paquay, Allan.Ostergaard}@esa.int

***Abstract*— An accurate and efficient numerical model is developed to simulate the far field of an antenna under test (AUT) measured in a Compact Antenna Test Range (CATR), on the basis of the known quiet zone field and the theoretical aperture field distribution of the AUT. The comparison with the theoretical far-field pattern of the AUT shows the expected measurement accuracy. The numerical model takes into account the relative movement of the AUT within the quiet zone and is valid for any CATR and AUT of which the quiet zone and aperture field, respectively, are known.**
The antenna under test in this study is the Validation Standard Antenna (VAST12), especially designed in the past for antenna test ranges validations. Simulated results as well as real measurements data are provided.

I. INTRODUCTION

Compact Antenna Test Ranges are widely used measurement facilities for antenna gain and pattern measurements. When measured in receive mode, the antenna under test is illuminated by a known incident quasi-planar wave, called quiet zone field, generated by the single or double reflector system of the CATR. CATR measurements have the big advantage of not needing probe correction and near-to-far field transformation, as it is the case for spherical, cylindrical or planar near-field antenna measurements. This apparently advantageous characteristic is, however, one of the major drawbacks of CATR systems, due to the lack of a well-defined procedure to evaluate the accuracy of the measured AUT pattern.

It is well known that an antenna pattern measured in a CATR is the result of the interaction between the AUT aperture field and the field distribution in the quiet zone of the CATR, see Fig. 1. Under ideal conditions, the quiet zone field distribution is a perfect plane wave with uniform amplitude and phase. In practice, the quality of the feed, the diffraction from the edges of the reflectors and the non-perfect absorbers in the facility introduce ripples in the uniform distribution of the quiet zone field, which affect the measured AUT pattern.

Several studies have been conducted in the past with the aim of modelling the quiet zone imperfections and estimate its influence on the measured AUT field. In [1] and [2] the effect of a non ideal quiet zone field on the AUT measured pattern was calculated by the coupling between the PO currents on the CATR reflectors and the AUT. The comparison between the AUT pattern obtained by coupling analysis and the ideal simulated pattern clearly showed the effect of the diffraction from the reflector serrations at the angles where the AUT main beam intercepted the reflector edges.

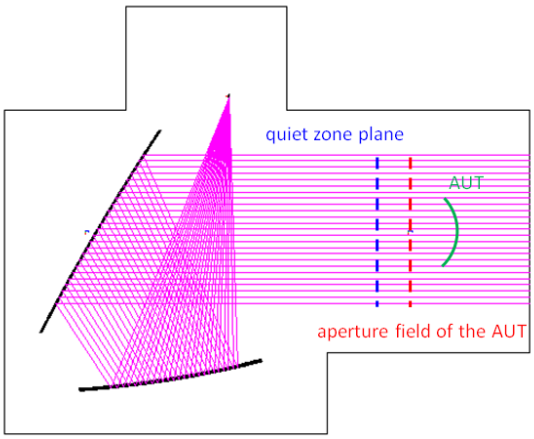

Fig. 1- A typical CATR with the quiet zone field and the AUT aperture field highlighted.

This effect, which is the main source of error in CATR measurements, was also observed and studied in detail by Philippakis [3] by developing a 3D model of the coupling between the AUT and the CATR quiet zone. The work was based on the coupling equation involving the plane wave spectra of the AUT and the CATR, but was applied only to analytical CATR and AUT distributions and was simplified to a 2D version, due to computational reasons. Though simple in its mathematical form and already presented in [4], the coupling equation requires both an efficient algorithm, in order to make the computation of practical use, and a good knowledge of the coupling phenomena in order to discriminate between the possible sources of errors.

The purpose of this work is to develop an accurate, general and efficient numerical model, called CATREP, able to compute the expected measurement accuracy of a CATR range, on the basis of the knowledge of the field in the quiet

zone and at the aperture distribution of the AUT, see Fig. 1. The model is based on the coupling equation and takes into account the relative movement of the AUT within the quiet zone field. More specifically, CATREP reads as input the quiet zone distribution and the AUT aperture field, and computes the ideal far-field of the AUT and the coupling between the AUT and the CATR. From the comparison of the ideal antenna pattern and the coupling pattern, the measurement accuracy of the CATR will be assessed. It is noted that the tool is not intended to provide a correction to the measured field, but identify the measurement errors which should be expected for a certain AUT, in a certain CATR.

The paper is organized as follows: in Section II the coupling theory is briefly summarized and the proposed algorithm is described, in Section III the approach is applied to the Validation Standard Antenna (VAST12) illuminated by an ideal and uniform quiet zone field, while in Section IV the technique is validated by real measurement data.

II. CATREP ALGORITHM: THEORY, IMPLEMENTATION AND WORKING PRINCIPLES

The mutual coupling between two antennas, one transmitting and one receiving, arbitrarily oriented and separated in free space is given by the so called coupling equation [5], which is based on the dot product and successive integration of the far fields of the two antennas.

By considering the CATR receiving and the AUT transmitting, the coupling equation can be written as

$$a_{CATR} = -\frac{1}{2k^2\zeta\sqrt{4\pi}}\int_{\Omega}\bar{E}_{far,CATR}(\bar{k})\cdot \bar{E}_{far,AUT}(-\bar{k})e^{-j\bar{k}\cdot\bar{r}_0}d\omega \qquad (1)$$

with k being the wavenumber, $\bar{k}$ the propagation vector $\bar{k} = k\sin\theta\cos\phi\hat{x} + k\sin\theta\sin\phi\hat{y} + k\cos\theta\hat{z}$ and ζ the free space impedance. The hemisphere expressed in function of the traditional $\theta\phi$ spherical coordinates is Ω. The signal a_{CATR} is the complex coupling pattern. It represents the AUT pattern measured in the CATR and is a function of the scanning grid coordinates. The vector $\bar{r}_0$ goes from the origin of the CATR coordinate system to the origin of the AUT coordinate system as illustrated in Fig. 2. It is noted that due to reciprocity, the role of the receiving and transmitting antenna can be interchanged, and that in Eq. 1 both patterns are assumed to be normalized to a total power of 4π watt, such that the output $\left|a_{CATR}\right|^2$ is the power received by the CATR when the AUT radiates a power of 4π watt. In order to compute Eq. 1, the CATR is assumed to be fixed in space, whereas the AUT is rotated on the given scanning grid, and for each AUT orientation the integral is computed. It is noted that to perform the integral of Eq. 1, the far-field patterns of the AUT and CATR must be expressed in the same coordinate system.

The far-field patterns of the AUT and CATR are computed from the respective aperture fields $\bar{E}_a$, which are input to CATREP, through the corresponding equivalent magnetic currents $\bar{J}_m$

$$\bar{J}_m = -2\hat{z}\times\bar{E}_a \qquad (2)$$

and the radiation integral [6]

$$\bar{E}_{far} = \frac{jk^2}{4\pi}\hat{r}\times\iint_a \bar{J}_m e^{jk(xu+yv)}dxdy \qquad (3)$$

where the integral is calculated over the aperture plane and $u = \sin\theta\cos\phi$, $v = \sin\theta\sin\phi$, with $\theta\phi$ describing the forward hemisphere. To obtain a fast algorithm, expanding the aperture fields in a Fourier series and computing analytically the far-fields from the Fourier coefficients was found to be the most successful approach.

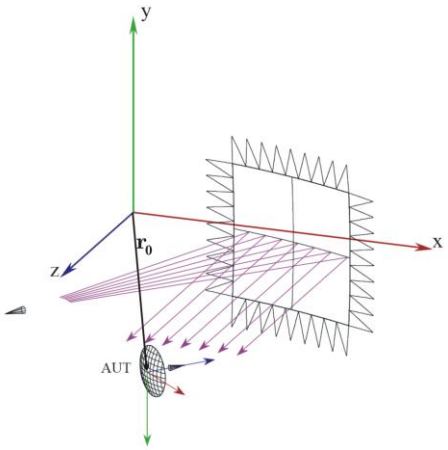

Fig. 2 – Coupling between the CATR and the AUT: AUT and CATR coordinate systems.

It has to be remembered that the radiation from the equivalent currents represents the antenna radiation provided that the field outside the aperture plane is negligible, otherwise incorrect diffractions will appear from the edges. However, a truncation of the aperture plane (especially of the quiet zone) can be accepted if the plane lies very close to the AUT, see Fig. 3.

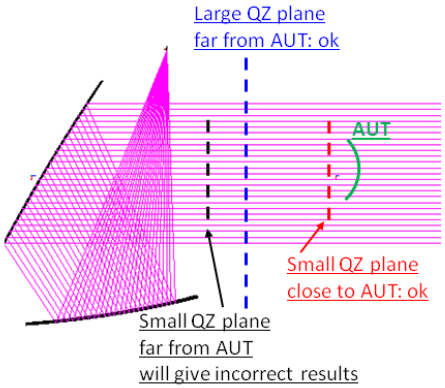

Fig. 3 – Acceptable and not acceptable QZ plane truncation.

In the numerical evaluation of Eq. 1, the integration is carried out in the CATR coordinate system and the solid angle element $d\omega$ is expressed as $d\omega = \sin\theta d\theta d\phi$. The directions of the diffracted rays depend on the rim of the CATR main reflector and its distance from the AUT: these can be found once the measurement set-up is known, see Fig. 4.

It is finally important to note that in practice a certain positioner determines one, and only one, type of scanning grid and one type of measured polarization, according to Table 1. This means that for a correct use of CATREP, i.e. to correctly model in CATREP the effects of a measurement, the choice of the field polarization and scanning grid has to be made on the basis of the antenna positioner available at the measurement facility of interest.

Positioner type	**Measured polarization**	**Scanning grid**
Roll/Az (DTU-pos.)	theta/phi	theta/phi
Ludwig 3rd	co/cx	co/cx
Az/El	El/Az	Az/El
El/Az	Az/El	El/Az

Table 1 - Relation between positioner type, measured polarization and scanning grids. At present, only the options written in red are available in CATREP.

III. SIMULATED RESULTS

A simple CATR quiet zone distribution was first considered. It was assumed that the CATR quiet zone field corresponded to the field radiated by a reflector of 7 by 5 meters, in the vertical and horizontal direction respectively, uniformly distributed in amplitude and phase. The origin of the CATR coordinate system $x_c y_c z_c$ was located at the center of the reflector, with x_c-axis horizontal and y_c-axis vertical, see Fig. 4, in such a way that the quiet field distribution coincided with the z_c=0 plane.

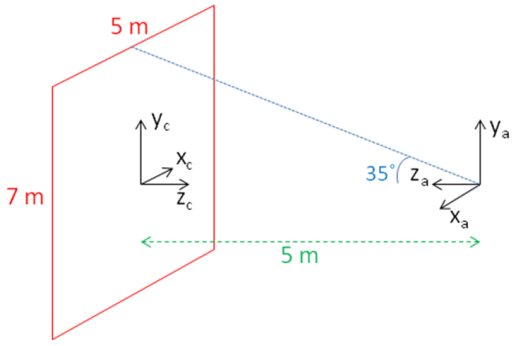

Fig. 4 – CATR main reflector, the coordinate system $x_c y_c z_c$ and the AUT coordinate system $x_a y_a z_a$.

The AUT was constituted by the VAST12 antenna, see Fig. 5. It consists of an offset shaped paraboloid working at 12 GHz, with circular projected aperture of diameter $D \approx 49$ cm $\approx 20\lambda$, and a rigid mounting structure. The antenna was designed in the nineties with the purpose of providing a stiff, robust and lightweight antenna with a number of interesting electrical properties, challenging and general enough to be tested in different measurement facilities [7].

A model of the VAST12 antenna was made with GRASP and the field radiated by the antenna was computed on the 120cm x 120cm plane located at d=51 cm from the center of the reflector, see Fig. 5, with physical optics on the reflector and method of moments on the mounting structure and the external surface of the feed horn. A plot of the obtained y-component is given in Fig. 6. It is noted that the $x_a y_a z_a$ coordinate system depicted in Fig. 5 coincides with the one shown in Fig. 4.

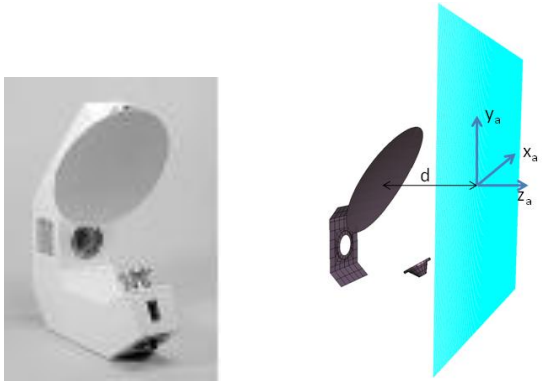

Fig. 5 – On the left, the VAST12 antenna, and on the right the GRASP model and the aperture plane where the field is computed.

The uniform field of the CATR at z_c=0 and the VAST12 antenna aperture field at z_a=0 were thus read by CATREP and the ideal far-field and the coupling between the antenna and the CATR were computed. Results can be seen in Fig. 7 for the amplitude of the co- polar component in dB on the cut ϕ= 90˚, for the case in which the CATR quiet zone is linearly polarized along y_c. It can be seen that the coupling pattern coincides with the expected far-field in the main lobe and first sidelobes except for a clear sidelobe error around the angles where the AUT main lobe intercepts the CATR rim, i.e. at $\theta \approx$ 35˚for ϕ=90˚, see Fig. 4. Similar results were obtained for the cut ϕ= 0˚. The sidelobe error is due to the abrupt field truncation on the planar reflector, which generates ripples in the corresponding far-field. These ripples affect the coupling pattern and show up as large sidelobe errors at the angles where the AUT main beam intercepts the reflector rim.

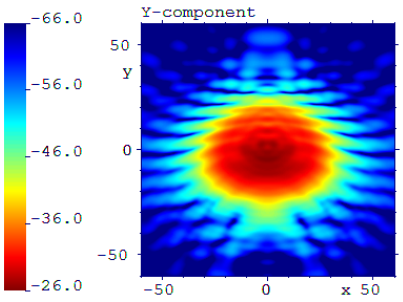

Fig. 6 – Amplitude of the y-component of the VAST12 antenna field on the aperture plane of Fig. 5.

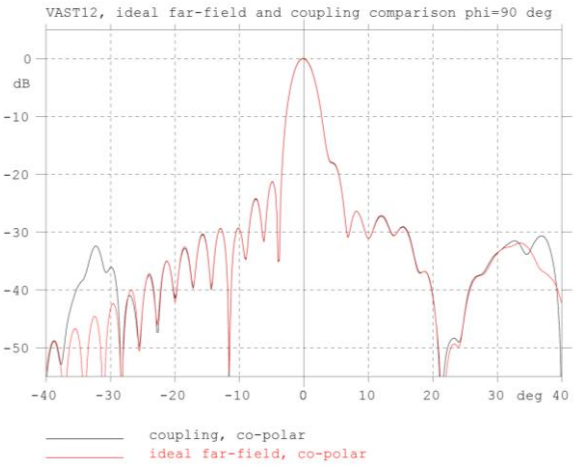

Fig. 7 – Amplitude of the far-field and coupling pattern for a uniform CATR distribution and the VAST12 antenna.

IV. EXPERIMENTAL RESULTS

The quiet zone field was then substituted by the field distribution measured in the ESTEC CPTR (Compact Payload Test Range), see Fig. 8 for a plot of the amplitude of the *y*-component. The CPTR quiet zone was measured by ESTEC in an indirect way, i.e. by transforming to the quiet zone plane the RCS pattern of a flat mirror of 1 m radius. It is noted that the method does not provide cross-polar information of the quiet zone field, and that only the *y*-component was available while the *x*-component was assumed to be zero. It is finally reminded that such a quiet zone field distribution only describes the quiet zone field of the CPTR in a circular area of 1 m radius, see Fig. 8, corresponding to the size of the mirror used to perform the quiet zone measurement. Though in practice the quiet zone field distribution of the ESTEC CPTR has a radius almost one meter wider, the knowledge of the QZ over the limited 1m radius area does not affect the results of CATREP, due to its vicinity to the AUT aperture plane, see Fig. 9 and Fig. 3.

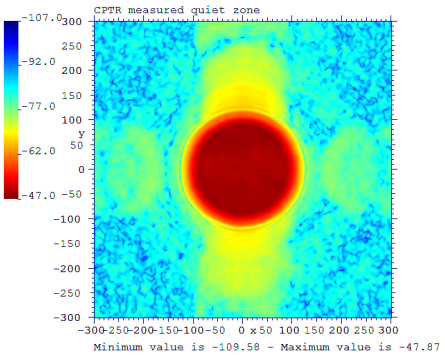

Fig. 8 - Amplitude of the *y*-component of the quiet zone field measured in the CPTR, (*xy*-plane in cm).

The CPTR geometry is shown in Fig. 9. The main reflector has a dimension of 8800 mm x 7500 mm, including serrations, where D_{CATR}=8800 mm. The distance *d* between the centre of the main reflector and the origin of the quiet zone coordinate system is *d*=17777 mm. The VAST12 coordinate system $x_a y_a z_a$ is oriented as in Fig. 5. The distance between the origin of the VAST12 and CPTR coordinate systems is equal to d_2=274.125 mm.

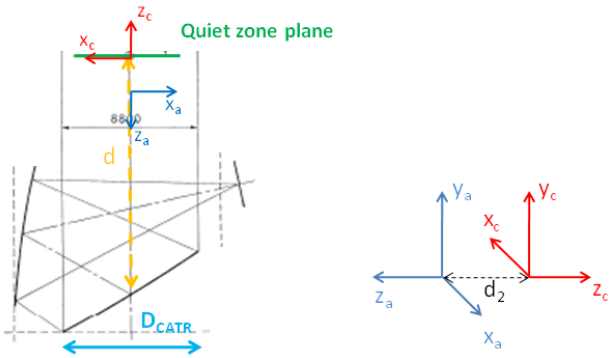

Fig. 9 – CPTR geometry (the distance between the coordinate systems is not to scale), and the VAST12 $x_a y_a z_a$ and CPTR $x_c y_c z_c$ coordinate systems.

A drawing of the positioner used in the ESTEC CPTR is given in Fig. 10. It consists of an elevation over azimuth positioner with elevation and azimuth axes not intersecting. By looking at Table 1, it can be seen that CATREP cannot right now correctly describe the movement of the AUT during a measurement in the ESTEC CPTR, since the AUT positioner of the ESTEC CPTR cannot be fully given as input to the program and the measured polarization is not implemented. It is however true that the azimuth over elevation polarization unit vectors can be approximated for small scanning angles to the co- and cross-polar unit vectors of Ludwig's third definition, which are on the other hand available in CATREP. On the two principal cuts ϕ=0° and ϕ=90° this approximation becomes exact.

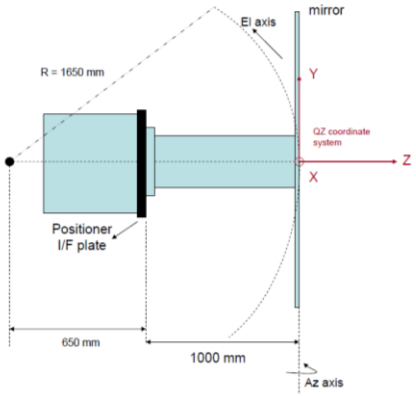

Fig. 10 – AUT positioner at the ESTEC CPTR.

The obtained co-polar patterns at φ=90° are shown in Fig. 11, normalized to their maxima, together with the difference pattern in blue. It can be seen that the main lobe and sidelobes coincide a part from the region around ±8°, where the coupling pattern is slightly higher. The difference pattern shows peaks around -40 dB in the ±8° domain, and decreases outside that domain.

Fig. 11 can be compared to the coupling pattern of Fig. 7 obtained for a uniform quiet zone field distribution. Though the geometrical set-up is different important observations can

be made. We can notice that sidelobe errors exist in both coupling patterns. These errors are at (or close to) the angles where the AUT main beam intercepts the (CPTR) reflector rim. For the coupling given by the quiet zone measured by ESTEC, these angles were estimated to be around ±8˚. For a uniform quiet zone field and a reflector with straight rim, the error is highly concentrated around this defined angular direction, while its influence is smaller when a quiet zone field coming from a reflector with serrations and tapered illumination is considered. Serrations together with the tapered illumination of the reflectors decrease the current distributions on the reflector close to the rim, and thus the diffraction from the edges.

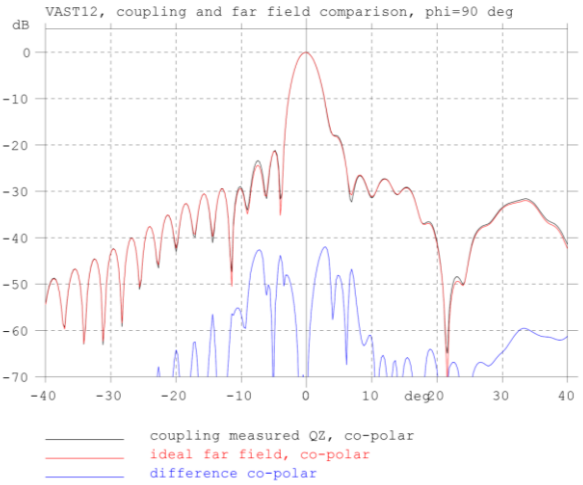

Fig. 11 - Coupling and far-field pattern obtained by CATREP with measured quiet zone data.

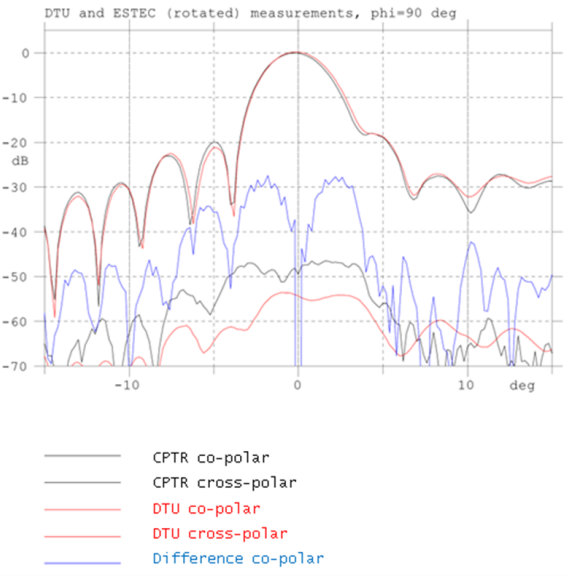

Fig. 12- Measurement pattern of the VAST12 antenna obtained at the DTU-ESA spherical near-field facility and at the ESTEC CPTR

Results obtained by CATREP were finally compared with measurements of the VAST12 antenna performed at the DTU-ESA spherical near-field antenna test facility (considered as exact measurement), and at the ESTEC CPTR, see Fig. 12, on the ±15˚ angular domain. By comparing Fig. 11 with Fig. 12, and especially the difference pattern which is not affected by the ideal and real VAST12 antenna, we can first observe a shift for the CPTR measurement with respect to the DTU measurement and CATREP results. We can then see that the difference pattern is generally higher (-30 dB) for the DTU-CPTR measurements, than for CATREP (-40 dB), and that this is due to the shift in the CPTR chamber. However, though the difference in the sidelobes is not the same, the angular domains at which they appear agree.

V. Conclusions

A general, accurate and efficient numerical model was developed to simulate the far field of an antenna under test measured in a Compact Antenna Test Range, on the basis of the coupling between the known quiet zone field of the CATR and the theoretical aperture field distribution of the AUT. The model takes into account the relative movement of the AUT during the measurement process. The theory behind the numerical model was summarized and the working principles of the algorithm were explained.

The AUT was constituted by the VAST12 antenna, and its aperture field was computed with GRASP. The quiet zone field was first considered ideal and uniform, and later substituted by a measured distribution. In both cases the comparison between the ideal AUT far-field and the coupling pattern clearly showed the inaccuracies introduced by a CATR measurement, given by sidelobes errors at the angle where the AUT main beam intercepts the CPTR reflector rim. These errors are significant, but concentrated in space, for a uniform quiet zone distribution, while decrease in amplitude for a quiet zone coming from a reflector with tapered illumination and serrations. CATREP results were finally confirmed by measurements of the VAST12 antenna.

Acknowledgment

This work was supported by the European Space Agency under the contract number 22106/08/NL/ST.

References

[1] Jensen, F., Giauffret, L., Marti-Canales, J., “Modeling of compact range quite zone fields by PO and GTD”, Proceedings of Antenna Measurements Technique Association, Symposium, AMTA, Monterey Bay, USA, pp. 242-247, October 1999.

[2] Jensen, F., Pontoppidan, K., “Modeling of the antenna-to-range coupling for a compact range”, Proceedings of Antenna Measurements Technique Association, Symposium, AMTA, Denver, CO, USA, pp. 387-391, October 2001.

[3] Philippakis, M., Parini, C. G., “Compact antenna range performance evaluation using simulated pattern measurements”, IEE Proc. Microw. Antennas Propag., Vol. 143, No. 3, June 1996, pp. 200-206.

[4] Yaghjian, A. D., “Efficient computation of antenna coupling and fields within the near-field region”, IEEE Transactions on Antennas and Propagation, Vol. AP-30, No. 1, Jan. 1982, pp. 113-128.

[5] Kerns, M. D., “Plane-wave scattering matrix theory of antennas and antenna-antenna interactions”, Nat. Bur. Stand. Monograph 162, June 1981.

[6] Collin, R.E., Zucker, F. J., *Antenna Theory, Part I*, McGraw Hill, 1969.

[7] Hansen, J. E., “Definition, design, manufacture, test use of a 12 GHz Validation Standard Antenna”, Technical report R672, EMI, Technical University of Denmark, October 1997.